We are IntechOpen, the world's leading publisher of Open Access books Built by scientists, for scientists

6,900
Open access books available

186,000
International authors and editors

200M
Downloads

Our authors are among the

154
Countries delivered to

TOP 1%
most cited scientists

12.2%
Contributors from top 500 universities

WEB OF SCIENCE™

Selection of our books indexed in the Book Citation Index in Web of Science™ Core Collection (BKCI)

Interested in publishing with us?
Contact book.department@intechopen.com

Numbers displayed above are based on latest data collected.
For more information visit www.intechopen.com

13

Optimal Gait Generation in Biped Locomotion of Humanoid Robot to Improve Walking Speed

Hanafiah Yussof[1], Mitsuhiro Yamano[2], Yasuo Nasu[2] and Masahiro Ohka[3]
[1]*Faculty of Mechanical Engineering, Universiti Teknologi MARA,*
[2]*Faculty of Engineering, Yamagata University*
[3]*Graduate School of Information Science, Nagoya University*
[1]*Malaysia*
[2,3]*Japan*

1. Introduction

Humanoid robot is a type of robot that the overall appearance is based on that of the human body. Humanoid robots include a rich diversity of projects where perception, processing and action are embodied in a recognizably anthropomorphic form in order to emulate some subset of the physical, cognitive and social dimensions of the human body and experience. The research on humanoid robots spans from stability to optimal control, gait generation, human-robot and robot-robot communication (Konno et al., 1997) (Hirai et al, 1998) (Cheng et al., 2001). In addition, humanoid robots have been also used to understand better human motion and establish working coexistence of human and humanoid robot (Althaus et al., 2004).

Humanoid robot with two legs usually have problem to stabilize its biped walk motions. In fact, one of the most sophisticated forms of legged motion is that of biped gait locomotion. Human locomotion stands out among other forms of biped locomotion chiefly in terms of the dynamic systems point of view. This is due to the fact that during a significant part of the human walking motion, the moving body is not in static equilibrium.

Biped walking robot can be classified by its gait. There are two major research areas in biped walking robot: the static gait and dynamic gait. For a biped robot, two different situations arise in sequence during the walking motion: the statically stable double-support phase in which the whole structure of the robot is supported on both feet simultaneously, and the statically unstable single-support phase when only one foot is in contact with the ground, while the other foot is being transferred from back to front. Eventually, this type of walking pattern delays the walking speed. Moreover, joint structure design in robots does not permit flexible movement like that of human being. Indeed, one motor only can rotate in one direction. Even by reducing reduction-ratio can increase the motor rotation, it will eventually reduce the torque output which is not desirable for real-time operation. Therefore, a method to control sufficient walking speed in conjunction with the biped gait trajectory is inevitably important. This is because in real-time application, the robots are likely to be required to walk faster or slower according to situation that occurred during the operation.

This chapter presents analysis results of optimal gait trajectory generation in a biped humanoid robot. The work presented in this chapter is focusing on analysis to improve biped walk quality and speed by considering reduction-ratio at joint-motor system with other physical parameters in humanoid robot's body. The analysis utilized a 21-dofs humanoid robot *Bonten-Maru II* as experimental platform.

The early sections of this chapter presents the background and motivation of current research, followed by hardware structure and design characteristics of humanoid robot *Bonten-Maru II*. The next section presents the optimization of trajectory generation using inverse kinematics for 6-dofs humanoid robot legs. A simplified approach was implemented to solving inverse kinematics problems by classifying the robot leg's joints into several groups of joint coordinate frames. To describe translation and rotational relationship between adjacent joint links, a matrix method proposed by Denavit-Hartenberg (Denavit and Hartenberg, 1955) was employed, which systematically establishes a coordinate system for each link of an articulated chain. In addition, to perform a smooth and reliable gait, it is necessary to define step-length and foot-height during transferring one leg in one step walk. The step-length is a parameter value that can be adjusted and fixed in the control system. On the other hand, the foot-height is defined by applying ellipse formulation. Interpolation by time function of the leg's start and end points using ellipse formulation provide smooth trajectory pattern at each gait.

The final section presents analysis of biped walking speed by maintaining reduction-ratio value but consider step length, hip-joint height from ground and duty-ratio as experimental parameters. Eventually, it is easy to control the walking speed by reducing or increasing the reduction-ratio at the robot joint-motor system. However, in real-time operation it is desirable to have a stable and high reduction-ratio value in order to provide high torque output to the robot's manipulator during performing tasks, such as during object manipulation, avoiding obstacle, etc. Therefore the reduction-ratio is required to remain always at fixed and high value.

2. Background and motivation

To realize human-like walking robots, many researches about the biped locomotion robot have been archived especially in prototyping biped locomotion, biped legged control and optimal gait locomotion. In these researches, dynamic and stable walking can be realized. Vukobratovic (Vukobratovic et al. 1990) have investigated the walking dynamics and proposed Zero Moment Point (ZMP) as an index of walking stability. Meanwhile, Takanishi and Hirai (Takanishi et al., 1985, Hirai et al., 1998) have proposed methods of walking pattern synthesis based on the ZMP, and demonstrate walking motion and pattern synthesis with real humanoid robots. Meanwhile, the methods to realizing dynamic walking were presented in (Hasegawa et al., 2000, Lim et al., 2000). Other achievements are in prototyping biped locomotion, biped legged control and optimal gait locomotion (Goswani et al., 1997, Capi et al., 2003).

Input energy is another important index for natural walking motion. Eventually, the energy-optimal trajectory for highly non-linear equations of a complex robot is hard to find numerically. Recently, an evolutionary optimization method, such as evolutionary programming (EP), genetic algorithm (GA) and so on have been identified to find the optimal solutions in a non-linear system. In the research with *Bonten-Maru II*, Capi (Capi et al., 2003, Nasu et al., 2007) has proposed a real time generation of humanoid robot optimal

gait by using soft computing techniques. GA was employed to minimize the energy for humanoid robot gait. The Radial Basis Function Neural Networks (RBFNN) is used for real time gait generations, which are trained based on GA data.

In order to realize optimal gait generation, several studies have been reported related with walking speed of biped robot. For example Chevallereau & Aoustin (Chevallereau & Aoustin, 2001) have studied optimal reference trajectory for walking and running of a biped robot. Furthermore, Yamaguchi (Yamaguchi et al., 1993) have been using the ZMP as a criterion to distinguish the stability of walking for a biped walking robot which has a trunk. The authors introduce a control method of dynamic biped walking for a biped walking robot to compensate for the three-axis (pitch, roll and yaw-axis) moment on an arbitrary planned ZMP by trunk motion. The authors developed a biped walking robot and performed a walking experiment with the robot using the control method. The result was a fast dynamic biped walking at the walking speed of 0.54 s/ step with a 0.3 m step on a flat floor. This walking speed is about 50% faster than that with the robot which compensates for only the two-axis (pitch and roll-axis) moment by trunk motion. Meanwhile, control system that stabilizes running biped robot HRP-2LR has been proposed by Kajita (Kajita et al., 2005). The robot uses prescribed running pattern calculated by resolved momentum control, and a running controller stabilizes the system against disturbance.

Eventually, it is easy to control the walking speed by reducing or increasing the reduction-ratio at the robot joint-motor system. However, in real-time operation it is desirable to have a stable and high reduction-ratio value in order to provide high torque output to the robot's manipulator during performing tasks, such as during object manipulation, avoiding obstacle, etc.

3. Humanoid robot "*Bonten-Maru II*"

Motivated by the current state-of-the-art in humanoids research, we have previously developed a research prototype biped humanoid robot called *Bonten-Maru II*. The *Bonten-Maru II* appearance diagram and outer dimension are shown in Fig. 1. It is 1.25 [m] tall and weight 31.5 [kg], which similar to an eight or nine year old child. The *Bonten-Maru II* is a research prototype humanoid robot, and such has undergone some refinement as different research direction is considered. During the design process, some predefined degree of stiffness, accuracy, repeatability, mobility and other design factor have been taken into consideration.

The *Bonten-Maru II* was designed to mimic as much as human characteristic, especially for contribution of its joints. Figure 2 shows configuration of dofs in the robot body. The robot has total of 21 dof: 6 dof for each leg, 3 dof for each arm, 1 dof for waist and 2 dof for head. The high number of dof gives the *Bonten-Maru II* possibility to realize complex motions. Moreover, the distribution of dof which is very similar with humans gives advantages for the humanoid robot to attain human-like motion. Every joint is driven by DC servomotor with a rotary encoder and harmonic drive reduction system, and PC with Linux is utilized for control. Rotation angles of joints were recorded by the rotary encoder that installed at rear side of DC servomotor. The sampling frequency is 200 Hz. The power is supplied to each joint by timing belt and harmonic drive reduction system. Gear number at the DC servomotor side is 60; while at the harmonic drive side is 16. Therefore, it makes reduction ratio at the harmonic side to be 1:100, while overall reduction ratio is 1:333.

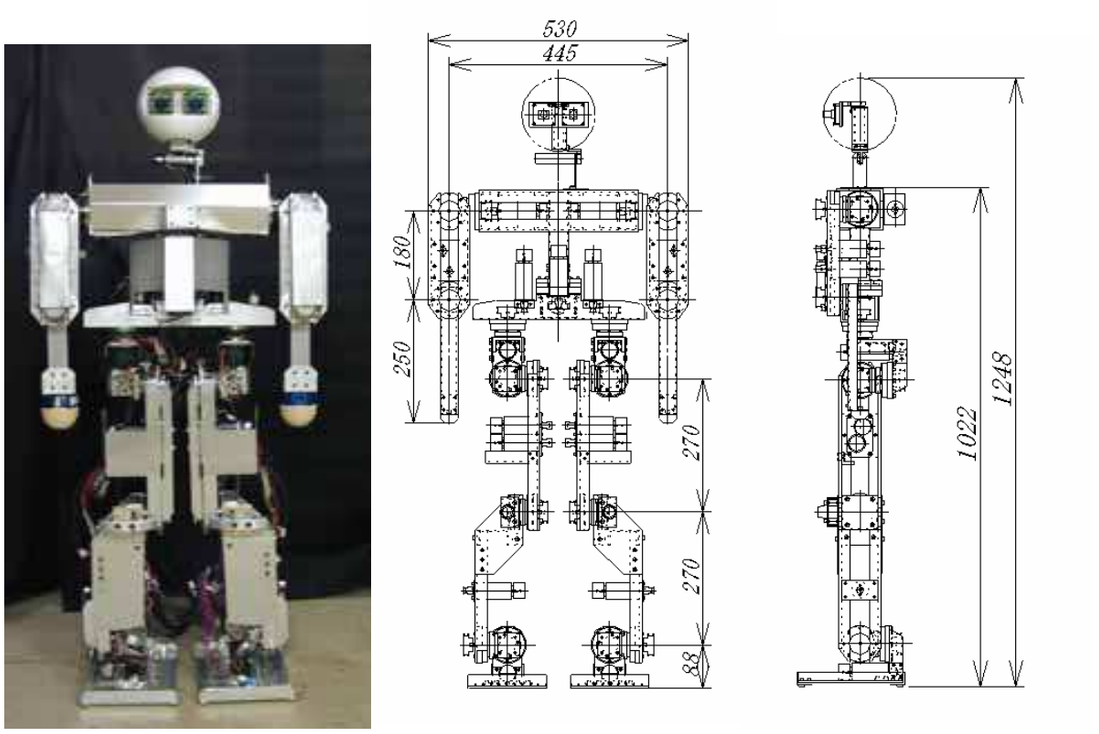

Fig. 1. *Bonten-Maru II* appearance diagram and outer dimension.

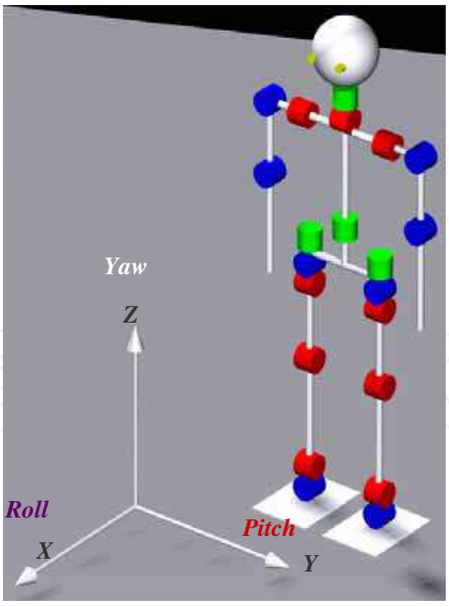

Fig. 2. Configuration of dofs in *Bonten-Maru II* humanoid robot body.

Table 1 shows range of joints rotation angle. Each joint has relatively wide range of rotation angle, especially for both leg's hip yaw which permit both legs to rotate in wide range of angle during correction of orientation and obstacle avoidance. Construction of the robot's links was also designed to mimic human's structure. The motor driver, the PC and the

power supply are placed outside of the robot. At the legs side, under each foot are four pressure sensor, two at the toe and two across the heel. These provide a good indication of both contact with the ground, and the Zero Moment Point (ZMP) position. At the head part is equipped with two monochrome CCD cameras (542x492 pixels) and connected to PC by video capture board.

Axis	Range of rotation angle (deg.)
Waist (yaw)	-45 ~ 45
Hip (yaw)	-90 ~ 90
Right hip (roll)	-90 ~ 25
Left hip (roll)	-25 ~ 90
Hip (pitch)	-130 ~ 45
Knee (pitch)	-20 ~150
Ankle (pitch)	-90 ~ 60
Right ankle (roll)	-90 ~ 20
Left ankle (roll)	-20 ~ 90

Table 1. Joint rotation range at leg system in *Bonten-Maru II*.

4. Optimization of trajectory generation in humanoid's legs

Optimization of trajectory generation is nacessary to ganerate optimal biped trajectory of humanoid robot legs. It is commonly known that trajectory of robot manipulator is obtain by solving kinematic relationship between adjacent links. Robot kinematics deals with the analytical study of the geometry of a robot's motion with respect to a fixed reference coordinate system as a function of time without regarding the force/ moments that cause the motion. Commonly, trajectory generation for biped locomotion robots is defined by solving forward and inverse kinematics problems (Kajita et al, 2005). In a forward kinematics problem, where the joint variable is given, it is easy to determine the end-effector's position and orientation. An inverse kinematics problem, however, in which each joint variable is determined by using end-effector position and orientation data, does not guarantee a closed-form solution.

Traditionally three methods are used to solve an inverse kinematics problem: geometric, iterative, and algebraic (Koker, 2005). However, the more complex the manipulator's joint structure, the more complicated and time-consuming these methods become. In order to optimize trajectory generation of biped walking robot, a simplified approach was proposed and implemented in 6-DOFs legs to solving inverse kinematics problems by classifying the robot's joints into several groups of joint coordinate frames at the robot's manipulator.To describe translation and rotational relationship between adjacent joint links, we employ a matrix method proposed by Denavit-Hartenberg (Denavit and Hartenberg, 1955), which systematically establishes a coordinate system for each link of an articulated chain. Optimization of kinematic solutions helps to increase calculation time and reduce memory usage of the robot control system. It also improve the stability of biped trajectory that can be utilize to ganerate and control the speed of biped walking.

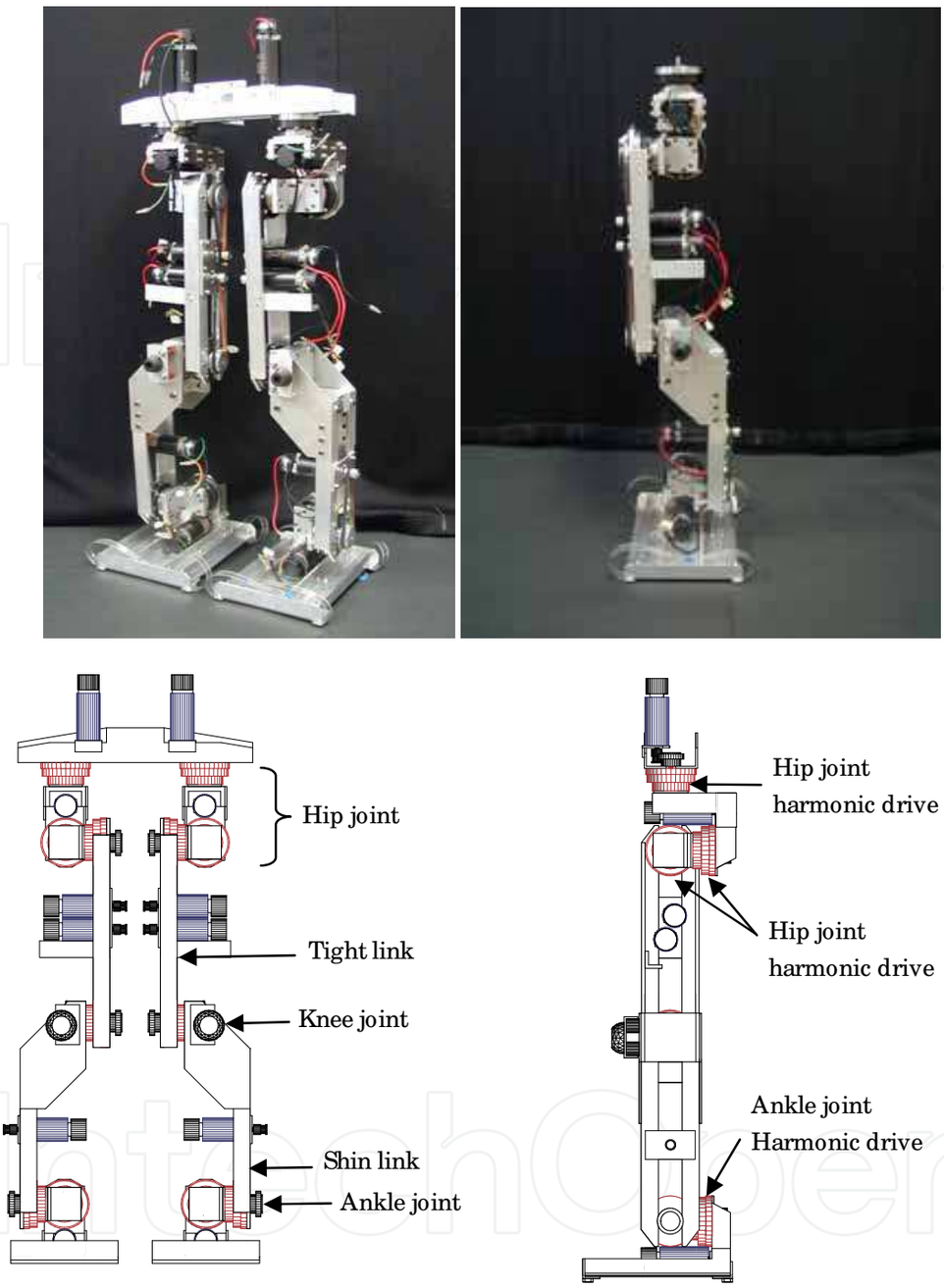

Fig. 3. Photograph of *Bonten-Maru II* lower side body and the configuration of links and joints.

4.1 Legs structure

Basic idea of legged robot is ability to perform wide and variety range of human-like gait motions. The *Bonten-Maru II* humanoid robot is designed to mimic as much as human structure, especially for its joints and links configuration to have wide range of rotation angle. Figure 3 shows photograph and diagram of the *Bonten-Maru II* lower side body.

Configuration of links, joints and harmonic drive at the *Bonten-Maru II* lower side body were shown in this figure. Each leg is consists of 6-dofs: 3 dof for hip, 1 dof for knee, and 2 dof for ankle. Hip-joint yaw is connecting each leg with the waist part.

The design of link position and joint-motor structure greatly influence the joint rotation range (Bischoff & Graefe, 2005). The link positions were configured with thigh link positioned at inner side of leg, while shin link positioned at outer side of the leg. It gives the hip joints wide rotation range to outside direction and the ankle joints also possible to rotate wider to inner side, at the same time gives better stability. Both of these links were connected with knee joint and were given specific space so that knee joint can rotate as far as 160 degree to back direction.

Configuration of the harmonic drive position at hip joints and ankle joints were installed at the rear side of roll direction so that the leg's link can swing to front direction in wide rotation angle. Moreover, both thigh links were given specific space so that when hip joint rotates to yawing direction, both links do not collide to each other. Consequently, rotation of hip joint at yaw direction can reach until 90 degree. In this research, wide rotation angle of yaw direction is required so that the robot can easily change its direction in wider angle, particularly during avoiding obstacles and operation in confined spaces.

4.2 Kinematics solutions of 6-DOFs Legs

Each of the legs in humanoid robot Bonten-Maru II has six DOFs: three DOFs (yaw, roll and pitch) at the hip joint, one DOF (pitch) at the knee joint and two DOFs (pitch and roll) at the ankle joint. In this research, only inverse kinematics calculations for the robot leg we solved. A reference coordinate is taken at the intersection point of the 3-DOF hip joint. In solving calculations of inverse kinematics for the leg, just as for arm, the joint coordinates are divided into eight separate coordinate frames as listed bellow.

Σ_0 : Reference coordinate.
Σ_1 : Hip yaw coordinate.
Σ_2 : Hip roll coordinate.
Σ_3 : Hip pitch coordinate.
Σ_4 : Knee pitch coordinate.
Σ_5 : Ankle pitch coordinate.
Σ_6 : Ankle roll coordinate.
Σ_h : Foot bottom-center coordinate.

Figure 4 shows a model of the robot leg that indicates the configurations and orientation of each set of joint coordinates. Here, link length for the thigh is l_1, while for the shin it is l_2. The Link parameters for the leg are defined in Table 2. Referring to Fig. 4, the transformation matrix at the bottom of the foot ($^{6}_{h}\mathbf{T}$) is an independent link parameter because the coordinate direction is changeable. Here, to simplify the calculations, the ankle joint is positioned so that the bottom of the foot settles on the floor surface. The leg's orientation is fixed from the reference coordinate so that the third row of the rotation matrix at the leg's end becomes like Eq. (1).

$$P_z\text{leg} = \begin{bmatrix} 0 & 0 & 1 \end{bmatrix}^T \tag{1}$$

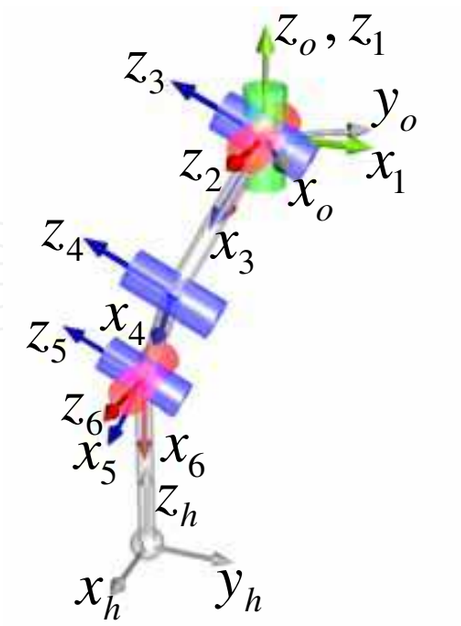

Fig. 4. Configurations of joint coordinates at the robot leg.

Link	$\theta_{i\text{leg}}$	d	α	l
0	$\theta_{1\text{leg}}+90^o$	0	0	0
1	$\theta_{2\text{leg}}-90^o$	0	90^o	0
2	$\theta_{3\text{leg}}$	0	90^o	0
3	$\theta_{4\text{leg}}$	0	0	l_1
4	$\theta_{5\text{leg}}$	0	0	l_2
5	$\theta_{6\text{leg}}$	0	-90^o	0
6	0	0	0	l_3

Table 2. Link parameters of the leg

Furthermore, the leg's links are classified into three groups to short-cut the calculations, where each group of links is calculated separately as follows.

i. From link 0 to link 1 (Reference coordinate to coordinate joint number 1).
ii. From link 1 to link 4 (Coordinate joint number 2 to coordinate joint number 4).
iii. From link 4 to link 6 (Coordinate joint number 5 to coordinate at the bottom of the foot).

Basically, i) is to control leg rotation at the Z-axis, ii) is to define the leg position, while iii) is to decide the leg's end-point orientation. A coordinate transformation matrix can be arranged as below.

$$ {}^{0}_{h}\mathrm{T} = {}^{0}_{1}\mathrm{T}\,{}^{1}_{4}\mathrm{T}\,{}^{4}_{h}\mathrm{T} = ({}^{0}_{h}\mathrm{T})({}^{1}_{2}\mathrm{T}\,{}^{2}_{3}\mathrm{T}\,{}^{3}_{4}\mathrm{T})({}^{4}_{5}\mathrm{T}\,{}^{5}_{6}\mathrm{T}\,{}^{6}_{h}\mathrm{T}) \quad (2) $$

Here, the coordinate transformation matrices for ${}^{1}_{4}\mathbf{T}$ and ${}^{4}_{h}\mathbf{T}$ can be defined as Eqs. (3) and (4), respectively.

$$ {}^{1}_{4}\mathbf{T} = {}^{1}_{2}\mathbf{T}\,{}^{2}_{3}\mathbf{T}\,{}^{3}_{4}\mathbf{T} = \begin{bmatrix} s_2c_{34} & -s_2s_{34} & -c_2 & l_1s_2c_3 \\ -s_{34} & -c_{34} & 0 & -l_1s_3 \\ -c_2c_{34} & c_2s_{34} & -s_2 & -l_1c_2c_3 \\ 0 & 0 & 0 & 1 \end{bmatrix} \tag{3} $$

$$ {}^{4}_{h}\mathbf{T} = {}^{4}_{5}\mathbf{T}\,{}^{5}_{6}\mathbf{T}\,{}^{6}_{h}\mathbf{T} = \begin{bmatrix} c_5c_6 & -c_5s_6 & -s_5 & l_2 + l_3c_5c_6 \\ s_5c_6 & -s_5s_6 & c_5 & l_3s_5c_6 \\ -s_6 & -c_6 & 0 & -l_3s_6 \\ 0 & 0 & 0 & 1 \end{bmatrix} \tag{4} $$

The coordinate transformation matrix for ${}^{0}_{h}\mathbf{T}$, which describes the leg's end-point position and orientation, can be shown with the following equation.

$$ {}^{0}_{h}\mathbf{T} = \begin{bmatrix} r_{11} & r_{12} & r_{13} & p_x \\ r_{21} & r_{22} & r_{23} & p_y \\ r_{31} & r_{32} & r_{33} & p_z \\ 0 & 0 & 0 & 1 \end{bmatrix} \tag{5} $$

From Eq. (1), the following conditions were satisfied.

$$ r_{13} = r_{23} = r_{31} = r_{32} = 0 \;,\; r_{33} = 1 \tag{6} $$

Hence, joint rotation angles $\theta_{1\text{leg}}$~$\theta_{6\text{leg}}$ can be defined by applying the above conditions. First, considering i), in order to provide rotation at the Z-axis, only the hip joint needs to rotate in the yaw direction, specifically by defining $\theta_{1\text{leg}}$. As mentioned earlier, the bottom of the foot settles on the floor surface; therefore, the rotation matrix for the leg's end-point measured from the reference coordinate can be defined by the following equation.

$$ {}^{0}_{h}\mathbf{R} = \mathrm{Rot}(z,\theta_{1\text{leg}}) = \begin{bmatrix} c\theta_{1\text{leg}} & -s\theta_{1\text{leg}} & 0 \\ s\theta_{1\text{leg}} & c\theta_{1\text{leg}} & 0 \\ 0 & 0 & 1 \end{bmatrix} = \begin{bmatrix} r_{11} & r_{12} & 0 \\ r_{21} & r_{22} & 0 \\ 0 & 0 & 1 \end{bmatrix} \tag{7} $$

Here, $\theta_{1\text{leg}}$ can be defined as below.

$$ \theta_{1\text{leg}} = \mathrm{atan2}\left(r_{21}, r_{22}\right) \tag{8} $$

Next, considering ii), from the obtained result of $\theta_{1\text{leg}}$, ${}^{0}_{h}\mathbf{T}$ is defined in Eq. (9).

$$ {}^{0}_{h}\mathbf{T} = \begin{bmatrix} -s_1 & -c_1 & 0 & P_{x\text{leg}} \\ c_1 & -s_1 & 0 & P_{y\text{leg}} \\ 0 & 0 & 1 & P_{z\text{leg}} \\ 0 & 0 & 0 & 1 \end{bmatrix} \tag{9} $$

Here, from constrain orientation of the leg's end point, the position vector of joint 5 is defined as follows in Eq. (10), and its relative connection with the matrix is defined in Eq. (11). Next, equation (12) is defined relatively.

$$ {}^{0}\mathbf{P}_5 = {}^{0}_{4}\mathbf{T}\,{}^{4}\mathbf{P}_5 = \begin{bmatrix} P_{x\text{leg}} & P_{y\text{leg}} & P_{z\text{leg}} - l_3 \end{bmatrix}^T , \tag{10} $$

$$ {}^{1}_{4}T\,{}^{4}\hat{P}_5 = {}^{0}_{1}T^{-1}\,{}^{0}\hat{P}_5 \tag{11} $$

$$ \begin{bmatrix} s_2c_{34} & -s_2s_{34} & -c_2 & l_1s_2c_3 \\ -s_{34} & -c_{34} & 0 & -l_1s_3 \\ -c_2c_{34} & c_2s_{34} & -s_2 & -l_1c_2c_3 \\ 0 & 0 & 0 & 1 \end{bmatrix} \begin{bmatrix} l_2 \\ 0 \\ 0 \\ 1 \end{bmatrix} = \begin{bmatrix} -s_1 & c_1 & 0 & 0 \\ -c_1 & -s_1 & 0 & 0 \\ 0 & 0 & 1 & 0 \\ 0 & 0 & 0 & 1 \end{bmatrix} \begin{bmatrix} p_x \\ p_y \\ p_z - l_3 \\ 1 \end{bmatrix} \tag{12} $$

$$ \text{Therefore,} \quad \begin{bmatrix} \hat{P}_{x_{\text{leg}}} \\ \hat{P}_{y_{\text{leg}}} \\ \hat{P}_{z_{\text{leg}}} \end{bmatrix} = \begin{bmatrix} s_2\left(l_1c_3 + l_2c_{34}\right) \\ -\left(l_1c_3 + l_2s_{34}\right) \\ -c_2\left(l_1c_3 + l_2c_{34}\right) \end{bmatrix}. \tag{13} $$

To define joint angles $\theta_{2\text{leg}}$, $\theta_{3\text{leg}}$, $\theta_{4\text{leg}}$, Eq. (13) is used . The rotation angles are defined as the following equations.

$$ \theta_{4_{\text{leg}}} = \text{atan2}\left(\pm\sqrt{1 - C^2}, C \right) \tag{14} $$

$$ \theta_{3_{\text{leg}}} = \text{atan2}\left(\hat{p}_{xz_{\text{leg}}}, \hat{p}_{y_{\text{leg}}} \right) + \text{atan2}\left(k_1, k_2 \right) \tag{15} $$

$$ \theta_{2_{\text{leg}}} = \text{atan2}\left(\hat{p}_{x_{\text{leg}}}, \hat{p}_{z_{\text{leg}}} \right) \tag{16} $$

Eventually, $C, \hat{p}_{xz_{\text{leg}}}, k_1, k_2$ are defined as follows.

$$ C = \frac{\hat{p}_{x_{\text{leg}}}{}^2 + \hat{p}_{y_{\text{leg}}}{}^2 + \hat{p}_{z_{\text{leg}}}{}^2 - (l_1{}^2 + l_2{}^2)}{2l_1l_2} \tag{17} $$

$$ \hat{p}_{xz_{\text{leg}}} = \sqrt{\hat{p}_{x_{\text{leg}}}{}^2 + \hat{p}_{z_{\text{leg}}}{}^2} \tag{18} $$

$$ k_1 = l_1 + l_2c_4, \;\; k_2 = -l_2s_4 \tag{19} $$

Finally, considering iii), joint angles $\theta_{5\text{leg}}$ and $\theta_{6\,\text{leg}}$ are defined geometrically by the following equations.

$$ \theta_{5\text{leg}} = -\theta_{3\text{leg}} - \theta_{4\text{leg}} \tag{20} $$

$$\theta_{6\text{leg}} = -\theta_{2\text{leg}} \tag{21}$$

4.3 Interpolation and gait trajectory pattern

Application of high degree of polynomial equations will help the manipulators to perform smooth trajectory. This method called interpolation. Interpolation refers to a time history of position, velocity and acceleration for each robotic joint. A common way of making a robot's manipulator to move from start point P_0 to end point P_f in a smooth, controlled fashion is to have each joint to move as specified by a smooth function of time t. Each joint starts and ends its motion at the same time, thus the robot's motion appears to be coordinated.

In order to compute these motions, in the case of position, velocity and acceleration at start point P_0 and end point P_f are given, interpolation of end-effector's position described in time t variable function was performed using polynomial equation to generate trajectory. In this research, we employ degree-5 polynomial equation as shown in Eq. (22) to solve interpolation from start point P_0 to end point P_f. Velocity and acceleration at P_0 and P_f are defined as zero; only the position factor is considered as a coefficient for performing interpolation.

$$P(t) = a_0 + a_1 t + a_2 t^2 + a_3 t^3 + a_4 t^4 + a_5 t^5 \tag{22}$$

Time factor at P_0 and P_f are describe as $t_0 = 0$ and t_f, respectively. Here, boundary condition for each position, velocity and acceleration at P_0 and P_f are shown at following equations.

$$\left.\begin{aligned}
&P(0) = a_0 = P_o \\
&\dot{P}(0) = a_1 = \dot{P}_o \\
&\dot{P}(0) = 2a_2 = \ddot{P}_o \\
&P(t_f) = a_0 + a_1 t_f + a_2 {t_f}^2 + a_3 {t_f}^3 + a_4 {t_f}^4 + a_5 {t_f}^5 = P_f \\
&\dot{P}(t_f) = a_1 + 2a_2 t_f + 3a_3 {t_f}^2 + 4a_4 {t_f}^3 + 5a_5 {t_f}^4 = \dot{P}_f \\
&\ddot{P}(t_f) = 2a_2 + 6a_3 t_f + 12a_4 {t_f}^2 + 20a_5 {t_f}^3 = \ddot{P}_f
\end{aligned}\right\} \tag{23}$$

Here, coefficient a_i (i = 0,1,2,3,4,5) are defined by solving deviations of above equations. Results of the deviations are shown at below Eq. (24).

$$\left.\begin{aligned}
a_0 &= y_o \\
a_1 &= \dot{y}_o \\
a_2 &= \frac{1}{2}\ddot{y}_o \\
a_3 &= \frac{1}{2{t_f}^3}\{20(y_f - y_0) - (8\dot{y}_f + 12\dot{y}_o)t_f + (\ddot{y}_f - 3\ddot{y}_o){t_f}^2\} \\
a_4 &= \frac{1}{2{t_f}^4}\{-30(y_f - y_o) + (14\dot{y}_f + 16\dot{y}_o)t_f - (2\ddot{y}_f - 3\ddot{y}_o){t_f}^2\} \\
a_5 &= \frac{1}{2{t_f}^5}\{12(y_f - y_o) - 6(\dot{y}_f + \dot{y}_o)t_f + (\ddot{y}_f - \ddot{y}_o){t_f}^2\}
\end{aligned}\right\} \tag{24}$$

As mentioned before, velocity and acceleration at P_0 and P_f were considered as zero, as shown in Eq. (25).

$$\dot{P}(0) = \ddot{P}(0) = \dot{P}(t_f) = \ddot{P}(t_f) = 0 \,. \tag{25}$$

Generation of motion trajectories from points P_0 to P_f only considered the position factor. Therefore, by given only positions data at P_0 and P_f, respectively described as y_0 and y_f, coefficients a_i (i = 0,1,2,3,4,5) were solved as below Eq. (26).

$$\left.\begin{aligned} a_0 &= y_o \\ a_1 &= 0 \\ a_2 &= 0 \\ a_3 &= \frac{10}{t_f^{\,3}}(y_f - y_o) \\ a_4 &= -\frac{15}{t_f^{\,4}}(y_f - y_o) \\ a_5 &= \frac{6}{t_f^{\,5}}(y_f - y_o) \end{aligned}\right\} \tag{26}$$

Finally, degree-5 polynomial function is defined as following equation.

$$y(t) = y_o + 10(y_f - y_o)u^3 - 15(y_f - y_o)u^4 + 6(y_f - y_o)u^5 \tag{27}$$

Where,

$$u = \frac{t}{t_f} = \frac{current\ time}{motion\ time} \,. \tag{28}$$

Meanwhile, to perform smooth and reliable gait trajectory in biped walk, it is necessary to define foot-height during transferring one leg in one step walk based on the acquired step-length. The foot-height is defined by applying ellipse formulation, like shown in gait trajectory pattern at Fig. 5. In walking forward and backward, the foot height at z-axis is defined in Eq. (29). Meanwhile during side-step walk, the foot height is defined in (30). Here, h is hip-joint height from the ground.

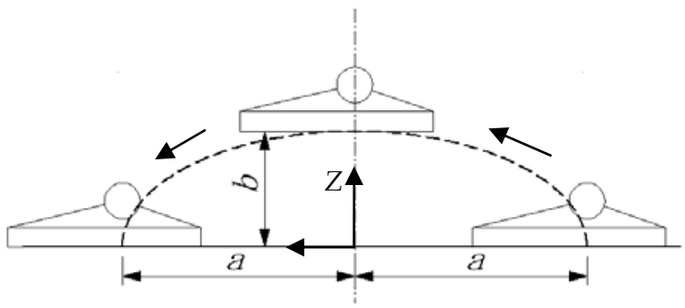

Fig. 5. Gait trajectory pattern of humanoid robot leg

$$z = b\left(1 - \frac{x^2}{S}\right)^{\frac{1}{2}} - h \tag{29}$$

$$z = b\left(1 - \frac{y^2}{S}\right)^{\frac{1}{2}} - h \tag{30}$$

In real-time operation, biped locomotion is performed by given the leg's end point position to the robot control system so that joint angle at each joint can be calculated by inverse kinematics formulations. Consequently the joint rotation speed and pattern is controlled by the above formulations of interpolation using degree-5 polynomial equations. By applying these formulations, each gait motion is performed in smooth and controlled trajectory.

4.4 Verification of biped trajectory generation by simulation

A simulation using animation that applies GnuPlot in humanoid robot *Bonten-Maru II* control system was performed to analyze and confirm of the robot joint's trajectory generation. Figure 6 presents the simulation interface of the robot's trajectory, which features a robot control process, a motion instructor process, and robot animation. In the

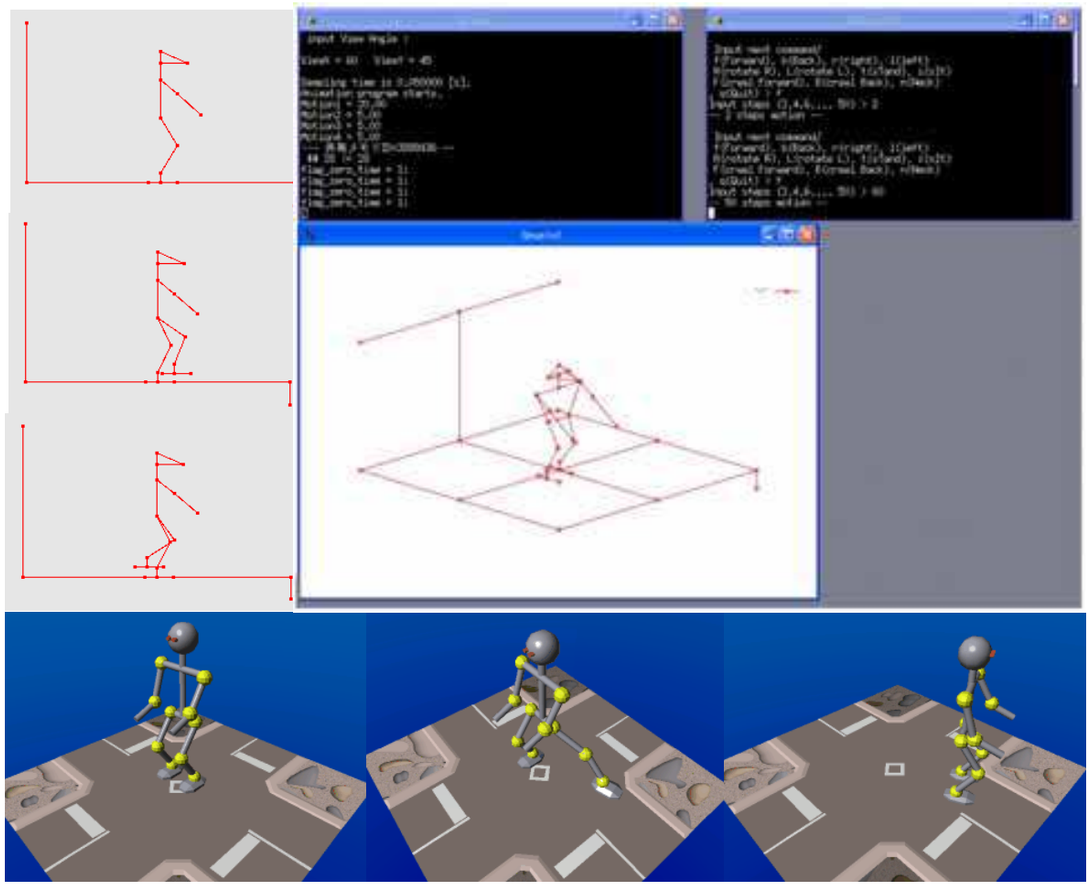

Fig. 6. Simulation interface presents robot's trajectory and motion process.

simulation, the robot performing biped locomotion of yawing motion to change its orientation by turning to back-left area.

In order to perform this motion, rotation of hip-joint yaw is the key-point. By solving Eq. (8), the robot rotation angle at hip joint is decided from *0* degree to *90* degree. Meanwhile target position of leg's end-point at *xyz*-axes plane is defined by solving inverse kinematics in Eqs. (14), (15), (16), (20), (21), and interpolation in Eq. (27). At this time the yawing angle θ_{1leg} is fixed at 70º.

During performing the yawing motion, at first the left leg's hip-joint yaw will rotate counterclockwise direction to θ_{1leg}. At the same time, the left leg follows along an ellipse trajectory in regard to *z*-axis direction to move the leg one step. This stepping motion is performed by given the leg's end point position to the robot's control system so that the joint angles of θ_{1leg}~θ_{6leg} could be solved by inverse kinematics calculations. The left leg position is defined by interpolation of the leg end point from its initial position with respect to the *xy*-axes position at a certain calculated distance. At this time the right leg acts as the support axis. Then, the robot corrects its orientation by changing the support axis to the left

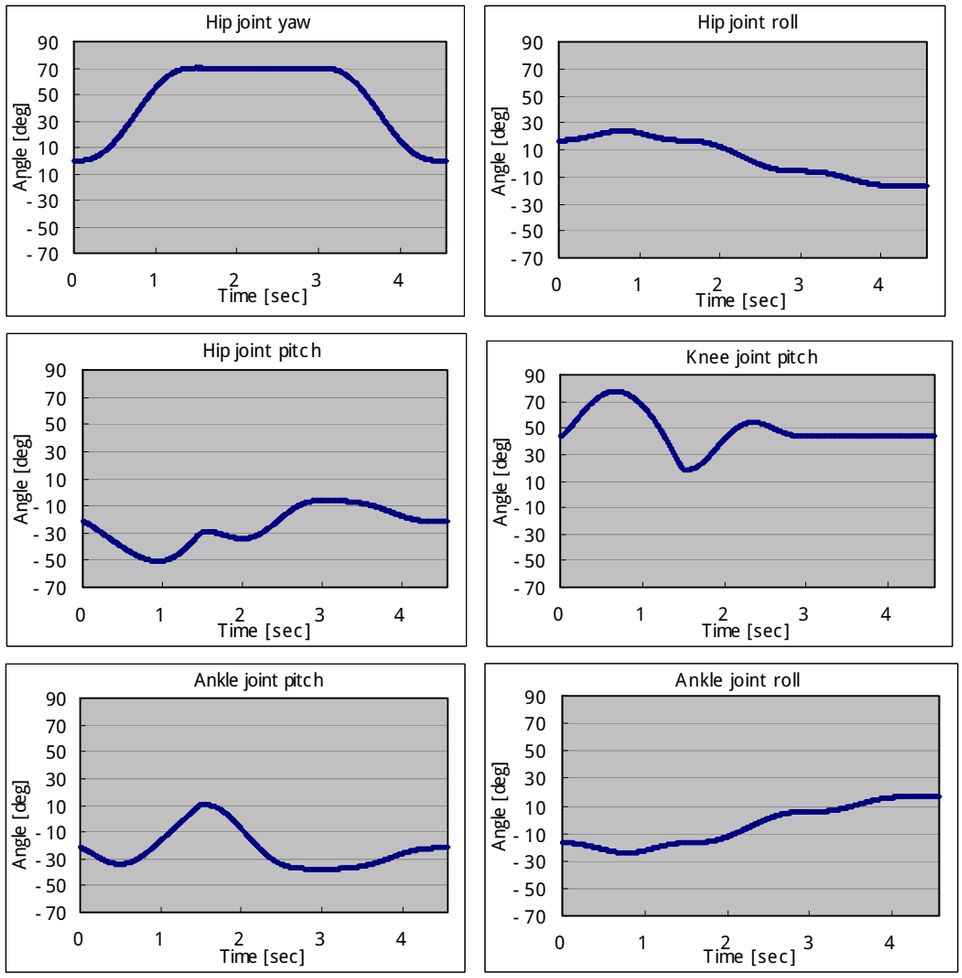

Fig. 7. Rotation angle of the left leg joints in biped walking while turning to left in yawing motion.

leg, while the left leg hip-joint yaw reverses the rotation to clockwise direction to complete the motion.

Each joint's rotation angles were saved and analyzed in a graph structure. For example, the graph for the left leg during yawing motion is plotted in Fig. 7. The graph shows the smooth trajectory of the rotation angles at each leg's joint. These simulation results verified reliability of the proposed kinematics and interpolation formulations to generate smooth and controlled trajectory for humanoid robot *Bonten-Maru II*.

5. Analysis of biped walking speed

5.1 Methodology

The main consideration in a biped humanoid robot is to generate the robot's efficient gait during performing tasks and maintain it in a stable condition until the tasks are completed. The efficiency in biped robots is normally related with how fast and how easy the tasks can be completed. In this research, to increase walking speed without changing the reduction-ratio, we considered three parameters to control the walking speed in biped robot locomotion:

1. ***Step length*; s**
2. hip-joint height from the ground; h
3. Duty-ratio; d

Figure 8 shows initial orientation of *Bonten-Maru II* during performing task which also indicate the step length and hip-joint height of the robot. The step-length is the distance between ankle-joints of a support leg and a swing leg when both of them are settled on the ground during walking motion. The hip-joint height is the distance between intersection point of hip-joint roll and pitch to the ground in walking position. Meanwhile, duty-ratio for biped robot mechanism is described as time ratio of one foot touches the ground when another foot swing to transfer the leg in one cycle of walking motion. In biped gait motion, two steps are equal to one cycle.

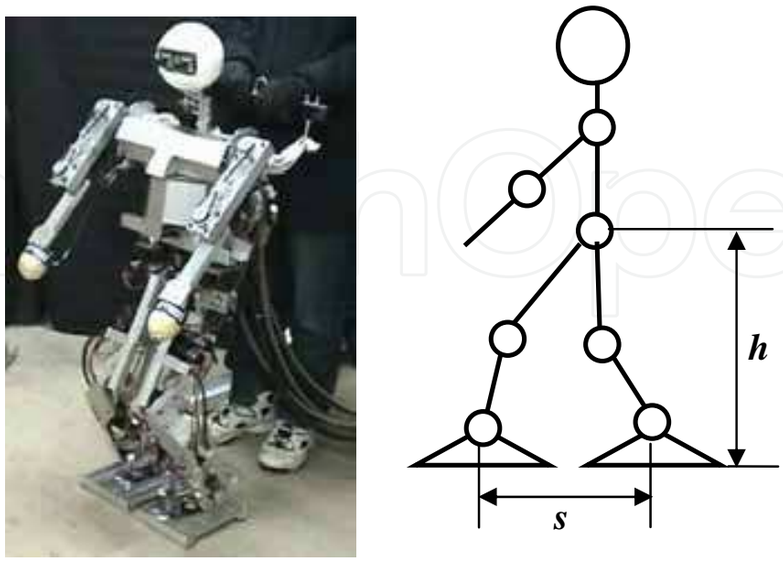

Fig. 8. Orientation of *Bonten-Maru II* to perform motion and parameters of hip-height h and step length s.

Hip-joint height [mm]	Max. step length in 1 step[mm]	Max. step length in 1 cycle [mm]
h_1=468	350	700
h_2=518	300	600
h_3=568	200	400

Table 3. Relationship of step length against hip-joint height at *Bonten-Maru II*.

Reffering to the *Bonten-Maru II* body and structure of the leg, the link parameters at the legs are used in calculations to define hip-joint height and maximum step length by geometrical analysis. Link parameters of the legs were calculated geometrically to define relation between step-length and hip-joint height. From the geometrical analysis, relation between the step-length and the hip-joint height is defined in Table 3.

At joint-motor system of *Bonten-Maru II*, maximum no-load rotation for the DC servomotor at each joint is 7220 [rpm]. This rotation is reduced by pulley and harmonic drive-reduction system to 1/ 333, in order to produce high torque output during performing tasks. We considered that the robot required high torque to perform tasks; therefore we do not change the reduction-ratio, which is 333:1. Eventually, these specifications produced maximum joint angular velocity at 130 [deg/ s]. However, for safety reason, the joint angular velocity at the motor was reduced to 117 [deg/ s]. The step time can be adjusted in the robot control system easily. However, if the step time is too small in order to increase walking speed, the robot motion becomes unstable. Moreover, the maximum step length performed becomes limited. In current condition, the step time for *Bonten-Maru II* to complete one cycle of walking is fixed between 7~10 second at maximum step length 75 [mm]. The duty-ratio d is increased gradually from 0.7 to 0.85. These parameter values are applied in simulation present in the next section.

5.2 Simulation analysis

A simulation analysis of the robot walking velocity using simulation interface that applies GnuPlot was performed based on parameters condition explained at previous section. The time for one circle of walking gait is initially fixed at 10 second. Each joint's rotation angles are saved and analyzed in a graph structure. Based on the joint angle, angular velocity of each joint was calculated.

Figure 9 shows joint angle data for right leg joints when performing 10 steps walk at condition: h=518 [mm], s=100 [mm] and d=0.7. From the angle data, angular velocity for each joint was calculated and presented in Fig. 10. The first and last gait shows acceleration and deceleration of the gait velocity. The three steps in the middle show maximum angular velocity of the legs joint.

Basically, in biped robot the maximum walking gait velocity is calculated from maximum joint angular velocity data by defining minimum step time for one gait. Eventually, by applying the same parameter, even if time for one step is initially different; the final joint angle obtained by the robot is same. Hence, in this analysis we can obtain the minimum step time in one step from the maximum joint angular velocity data that the initial step time was 10 seconds. Basically, the minimum gait time in one step is satisfying following equation:

$$t_{\min} < \frac{v_{\theta\max} \times 10}{V_{\theta\max}}. \tag{31}$$

Here, $V_{\theta\max}$ is the maximum joint angular velocity at the motor, t_{min} is minimum time for one step, and $v_{\theta max}$ is maximum joint angular velocity in each gait. Finally, the maximum walking gait velocity w_{max} is defined by dividing length s with minimum step time t_{min} in each gait, as shown in following equation.

$$w_{\min} = \frac{s}{t_{\min}} \tag{32}$$

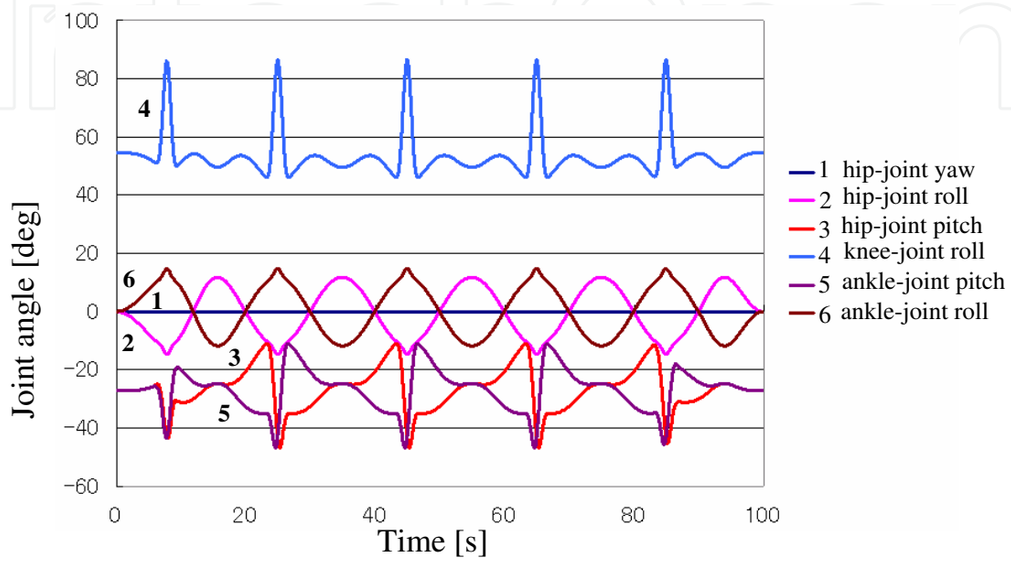

Fig. 9. Graph of joint rotation angle at right leg.

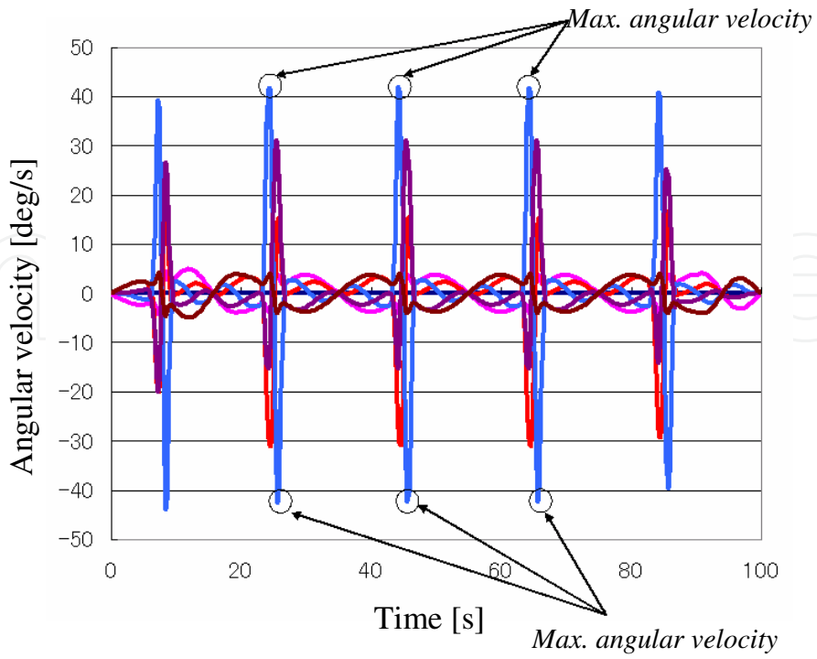

Fig. 10. Graph of angular velocity of joint rotation at right leg.

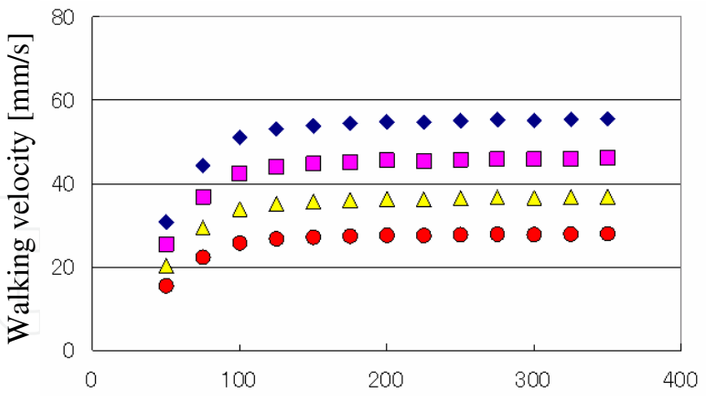

(a) Hip-joint height 468 [mm]

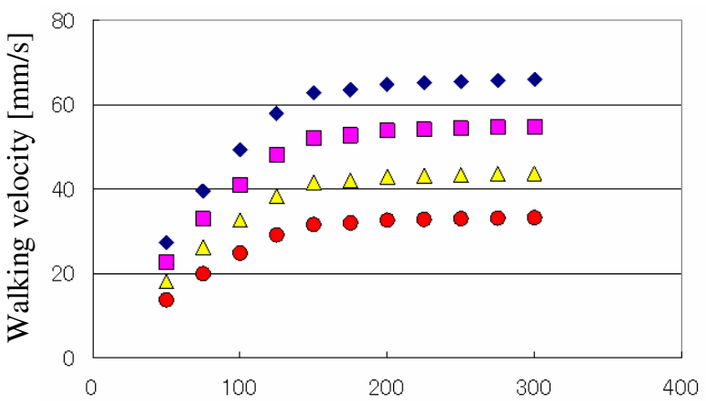

(b) Hip-joint height 518 [mm]

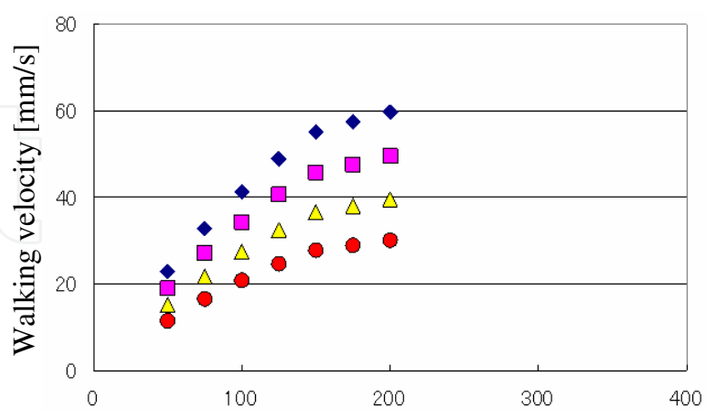

(c) Hip-joint height 568 [mm]

Duty-ratio: ◆:0.7, ■:0.75, △0.8, ●:0.85

Fig. 11. Analysis results of maximum walking velocity at each gait.

Simulation results of walking gait velocity at each parameters value are compiled in graphs as shown in Fig. 11(a), (b) and (c). According to these graphs, from the relation of walking velocity and step length, the walking velocity was maintain nearly at constant value when it reached certain step length. Moreover, in relation of step length and hip-joint height, the higher hip-joint position is providing wider step length to perform better walking distance.
At this point, lower duty-ratio shows the best results in relation of the hip-joint height and the step length for higher walking gait velocity, as shown in Fig. 11(b), where the low duty-ratio shows high walking velocity in relationship between the hip-joint-height and the step-length. It means by shorten the time for the support leg touching the ground will urge swing leg to increase its speed to complete one walking cycle, thus increase the walking velocity. At the same time, by choosing suitable step-length and hip-joint-height parameters, travel distance in each step can be improved. Analysis results revealed that it is possible to control biped walking speed without reducing the reduction-ratio at the joint-motor system.
From the simulation results, we can conclude that lower duty-ratio in suitable hip-joint height comparatively provided higher walking gait velocity. For *Bonten-Maru II*, the maximum walking gait velocity was improved from 30 [mm/ s] to 66 [mm/ s], which is about two times better than current walking velocity. At this time the hip-joint height is 518 [mm] and the time for one step is 4.5 seconds.

Fig. 12. Humanoid robot performs biped walking applying the best parameters value from simulation results: h=518 [mm], s=200 [mm] and d=0.7, time per step 4.5 sec.

Fig. 13. Humanoid robot performs biped walking applying current parameters value: h=568 [mm], s=75 [mm] and d=0.8, time per step 2.5 sec.

5.3 Experiments with *Bonten-Maru II*

Real-time experiments with the biped humanoid robot *Bonten-Maru II* were conducted to evaluate performance of the proposed methodology of optimal biped locomotion to improve walking speed of the humanoid robot. The parameter values that revealed the best result in simulation were applied, in comparison with current walking condition. Figures 12 and 13 respectively show photograph of the actual robot's walking motion in each experiment, which also indicate the parameter values applied. Travel distance was measured during the experiments.

The experimental results show that by applying the best parameters value obtained in the simulation results, the walking speed was improved. At the same time, the travel distance is longer about three times compared with current condition. This result reveals that the travel distance was improved in conjunction with the improvement of walking speed in the biped humanoid robot. The robot performed biped walking in smooth and stable condition.

5.3 Result and discussion

In our approach, we directly analyze geometrically the robot link structures and dimensions, and consider duty-ratio as effective parameters to improve walking speed in biped humanoid robot. Simulation results based on humanoid robot *Bonten-Maru II* parameters reveals that walking speed was improved by applying low duty-ratio at appropriate step length and hip-joint height. The walking speed increased about two times compared to normal condition. Meanwhile, real-time experiments utilizing real biped humanoid robot based on simulation results shows that the robot's travel distance during walking was improved about three times better than current walking condition. This analysis proved that it is possible to improve walking speed in stable biped locomotion without reducing the reduction-ratio.

6. Conclusion

This chapter presented analysis of biped gait locomotion to improve walking speed in humanoid robot without changing reduction-ratio at joint-motor system. Step length, hip-joint height, and duty-ratio were identified as parameters in this analysis. A Relationship between step length and hip-joint height was defined using geometrical calculations. Simulation analysis was conducted followed by real time experiments using humanoid robot *Bonten-Maru II*. Simulation results based on the humanoid robot *Bonten-Maru II* revealed that walking speed was improved by applying low duty-ratio at appropriate step length and hip-joint height. The walking speed increased about two times compared to normal condition. The real-time experiments utilizing *Bonten-Maru II* based on the simulation results shows that the robot's travel distance during walking was improved about three times better than current walking condition. The robot also walked faster in a stable condition compared to current walking condition.

This analysis proved that it is possible to improve walking speed in biped walking robots without reducing the reduction-ratio. The presented optimal gait generation in biped locomotion improved the performance of humanoid robot system towards operation in real world. This was proved by simulation and experimental results. Moreover, analysis results of gait trajectory generation proposed an efficient gait pattern for the biped robot. Since the analysis results revealed that it is possible to control biped locomotion speed without changing reduction-ratio at joint-motor system, the high torque output at robot's manipulator to conduct tasks in various motions is maintained.

7. Acknowledgement

Part of this study was supported by a fiscal 2006 Grant-in-Aid for Scientific Research in Exploratory Research from the Japan Ministry of Education, Culture, Sports, Science and Technology (Grant no. 18656079), and year 2008-2010 Grant-in-Research by the Japan Society for the Promotion of Science (JSPS) no. P08062. The authors are grateful with the support from Universiti Teknologi MARA.

8. References

Althaus, P., Ishiguro, H., Kanda, T., Miyashita T. & Christensen, H. I. (2004). Navigation for Human-Robot Interaction Tasks, *IEEE International Conference on Robotics and Automation (ICRA2004)*, pp. 1894-1900

Bischoff, R. & Graefe, V. (2005). Design principle for dependable robotics assistants, International Journal of Humanoid robotics, Vol. 1 (1), pp. 95-125

Capi, G., Nasu, Y., Mitobe K. & Barolli, L. (2003). Real time gait generation for autonomous humanoid robots: A case study for walking, *Journal Robotics and Autonomous Systems*, Vol. 42, No.2, pp. 169-178

Cheng, G., Nagakubo, A. & Kuniyoshi, Y. (2001). Continuous humanoid interaction: An integrated perspective -gaining adaptivity, redundancy, flexibility- in one, *Journal of Robotics and Autonomous Systems*, Vol. 37, Issues 2-3 pp 161-183

Chevallereau, C. & Aoustin, Y. (2001). Optimal trajectories for walking and running of a biped robot, Robotica, Vol. 19, Issue 5, pp. 557-569

Denavit, J. & Hartenberg, S. (1995). A kinematics notation for lower-pair mechanisms based upon matrices, *Journal of Applied Mechanics*, Vol. 77, pp. 215-221

Goswani, A., Espiau B., & Keramanie, A. (1997). Limit cycles in a passive compass gait biped and passivity-mimicking control laws, *Journal Autonomous Robots*, Vol. 4, pp. 273-286

Hasegawa, Y., Arakawa T. & Fukuda T. (2000). Trajectory generation for biped locomotion robot, *Journal Mechatronics*, Vol. 10, Issue 1-2, pp. 67-89

Hirai, K., Hirose, M., Haikawa, Y. & Takenaka, T. (1998). The development of Honda humanoid robot, *Proceedings of International Conference on Robotics and Automation'98*, pp. 1321-1326

Kajita, S., Nagasaki, T., Kaneko, K., Yokoi, K. & Tanie, K. (2005). A running controller of humanoid biped HRP-2LR, *Proceeding of the 2005 IEEE International Conference on Robotics and Automation (ICRA2005)*, pp. 618-624, Barcelona, Spain

Koker, R. (2005). Reliability-based approach to the inverse kinematics solution of robots using Elman's network, *Journal of Engineering Application of Artificial Intelligence*, Vol. 18, No. 6, pp. 685-693

Konno, A., Nagashima, K., Furukawa, R., Nishiwaki, K., Noda, T., Inaba M. & Inoue, H. (1997). Development of a humanoid robot Saika, *Proceeding of IEEE/RSJ Int. Conf. on Intelligent Robots and Systems (IROS'97)*, Grenoble, France, pp. 805-810

Lim, H., Yamamoto Y. & Takanishi, A. (2000). Control to realize human-like walking of a biped humanoid robot, *Proceeding of IEEE Int. Conf. System, Man and Cybernetics*, Vol. 5, pp. 3271-3276

Nasu, Y., Capi, G., Hanafiah Y., Yamano, M. & Ohka, M. (2007). Development of a CORBA-based humanoid robot and its applications, *Humanoid Robots*, by pro literature Verlag, Chapter 30, pp. 551-590

Takanishi, A., Ishida, M., Yamazaki, Y. & Kato, I. (1985). The realization of dynamic walking robot WL-10RD, *Proceedings of International Conference on Robotics and Automation (ICRA'85)*, pp. 459-466

Vukobratovic, M., Brovac, B., surla D. & Stokic, D. (1990). Biped locomotion, *Springer Verlag*

Yamaguchi, J., Takanishi, A. & Kato, I. (1993). Development of a biped walking robot compensating for three-axis moment by trunk motion, *Proceeding of 2003 EEE/RSJ International Conference on Intelligent Robots and Systems (IROS '93)*

IntechOpen

IntechOpen

Biped Robots

Edited by Prof. Armando Carlos Pina Filho

ISBN 978-953-307-216-6
Hard cover, 322 pages
Publisher InTech
Published online 04, February, 2011
Published in print edition February, 2011

Biped robots represent a very interesting research subject, with several particularities and scope topics, such as: mechanical design, gait simulation, patterns generation, kinematics, dynamics, equilibrium, stability, kinds of control, adaptability, biomechanics, cybernetics, and rehabilitation technologies. We have diverse problems related to these topics, making the study of biped robots a very complex subject, and many times the results of researches are not totally satisfactory. However, with scientific and technological advances, based on theoretical and experimental works, many researchers have collaborated in the evolution of the biped robots design, looking for to develop autonomous systems, as well as to help in rehabilitation technologies of human beings. Thus, this book intends to present some works related to the study of biped robots, developed by researchers worldwide.

How to reference

In order to correctly reference this scholarly work, feel free to copy and paste the following:

Hanafiah Yussof, Mitsuhiro Yamano, Yasuo Nasu and Masahiro Ohka (2011). Optimal Gait Generation in Biped Locomotion of Humanoid Robot to Improve Walking Speed, Biped Robots, Prof. Armando Carlos Pina Filho (Ed.), ISBN: 978-953-307-216-6, InTech, Available from: http://www.intechopen.com/books/biped-robots/optimal-gait-generation-in-biped-locomotion-of-humanoid-robot-to-improve-walking-speed

INTECH
open science | open minds

InTech Europe
University Campus STeP Ri
Slavka Krautzeka 83/A
51000 Rijeka, Croatia
Phone: +385 (51) 770 447
Fax: +385 (51) 686 166
www.intechopen.com

InTech China
Unit 405, Office Block, Hotel Equatorial Shanghai
No.65, Yan An Road (West), Shanghai, 200040, China
中国上海市延安西路65号上海国际贵都大饭店办公楼405单元
Phone: +86-21-62489820
Fax: +86-21-62489821

© 2011 The Author(s). Licensee IntechOpen. This chapter is distributed under the terms of the Creative Commons Attribution-NonCommercial-ShareAlike-3.0 License, which permits use, distribution and reproduction for non-commercial purposes, provided the original is properly cited and derivative works building on this content are distributed under the same license.

IntechOpen

IntechOpen